

Soil-geogrid interaction under cyclic and post-cyclic pullout loading conditions

Interaction sol-géogridde sous des conditions de chargement d'arrachement cycliques et post-cycliques

Fernanda Bessa Ferreira, Castorina Silva Vieira, Maria de Lurdes Lopes & Pedro Gil Ferreira
CONSTRUCT, Faculty of Engineering, University of Porto, Portugal, fbf@fe.up.pt

ABSTRACT: Geosynthetics have been widely used in geotechnical engineering practice to enhance the mechanical behaviour of permanent soil structures, such as road and railway embankments, retaining walls and steep slopes. When these reinforced systems are subjected to repeated loads, the characterisation of soil-geosynthetic interfaces under cyclic loading conditions is essential. In this study, a series of large-scale pullout tests has been conducted to evaluate the pullout response of a uniaxial geogrid embedded in a granite residual soil under cyclic and post-cyclic loading conditions. The influence of soil placement density, loading frequency and amplitude on the geogrid pullout behaviour was investigated by considering different soil densities and cyclic loading patterns. A comparison between the geogrid pullout resistance reached during the post-cyclic stage and that estimated from monotonic tests carried out under otherwise identical test conditions was then established. Test results have shown that soil density is a key factor affecting the geogrid deformation behaviour under cyclic loading, as well as the mobilised post-cyclic pullout resistance. The cumulative cyclic displacements of the reinforcement were found to decrease with increasing frequency and soil density, whereas in contrast, the loading amplitude adversely affected the accumulation of displacements over the geogrid length.

RÉSUMÉ: Les géosynthétiques ont été largement utilisés dans la pratique de l'ingénierie géotechnique pour améliorer le comportement mécanique des structures de sol permanentes, telles que les remblais routiers et ferroviaires, les murs de soutènement et les pentes raides. Lorsque ces systèmes renforcés sont soumis à des sollicitations répétées, la caractérisation des interfaces sol-géosynthétique sous chargement cycliques est indispensable. Dans cette étude, une série d'essais d'arrachement à grande échelle a été menée pour évaluer la réponse à l'arrachement d'une géogridde uniaxiale encastrée dans un sol résiduel granitique dans des conditions de chargement cycliques et post-cycliques. L'influence de la densité de mise en place du sol, de la fréquence du chargement et de l'amplitude sur le comportement d'arrachement de la géogridde a été étudiée en considérant différentes densités de sol et modèles de chargement cycliques. Une comparaison entre la résistance à l'arrachement de la géogridde atteinte pendant la phase post-cyclique et celle estimée à partir d'essais monotones effectués dans des conditions expérimentales par ailleurs identiques a ensuite été établie. Les résultats des tests ont montré que la densité du sol est un facteur clé affectant le comportement de déformation de la géogridde sous chargement cyclique, ainsi que la résistance à l'arrachement post-cyclique mobilisée. Les déplacements cycliques cumulés du renfort diminuent avec l'augmentation de la fréquence et de la densité du sol, alors qu'en revanche, l'amplitude de chargement affecte négativement l'accumulation des déplacements sur la longueur de la géogridde.

KEYWORDS: soil-geogrid interface, pullout test, cyclic and post-cyclic loading, amplitude, frequency.

1 INTRODUCTION

Knowledge about soil-geosynthetic interaction characteristics is required for the safe design and adequate performance of geosynthetic-reinforced soil structures, such as retaining walls, steep slopes, road and railway embankments and bridge abutments. Since these structures are often subjected to repeated loads due to road and railway traffic, waves and earthquakes (among others), the understanding of soil-geosynthetic interface behaviour under cyclic loading conditions is of great importance.

While the interaction between different soils and geosynthetics under monotonic pullout loading has been extensively investigated over the past few decades (Farrag et al. 1993, Lopes & Ladeira 1996a, 1996b, Palmeira 2004, Moraci and Gioffrè 2006, Moraci & Recalcati 2006, Khedkar & Mandal 2009, Huang & Bathurst 2009, Weerasekara & Wijewickreme 2010, Tran et al. 2013, Ferreira et al. 2016, 2020a), only limited effort has been expended to characterise the cyclic and post-cyclic pullout behaviour of geosynthetics (Raju & Fannin 1998, Moraci & Cardile 2009, 2012, Cardile et al. 2019, Ferreira et al. 2020b, Vieira et al. 2020a; Mahigir et al. 2021).

In view of this, a series of large-scale laboratory pullout tests has been conducted to evaluate the pullout response of a uniaxial extruded geogrid embedded in a well-graded granite residual soil under cyclic and post-cyclic loading conditions. The effects of

soil placement density, frequency and amplitude of the cyclic load on the reinforcement pullout resistance and associated displacements and strains are evaluated and discussed. To analyse the potential degradation of pullout resistance due to cyclic loading, a comparison is made between the maximum pullout forces mobilised during the post-cyclic loading stage and those obtained from monotonic (benchmark) tests performed under otherwise identical test conditions.

2 MATERIALS AND METHODS

2.1 Test apparatus

The large-scale pullout test rig used in this study was developed at the University of Porto during some previous research (Lopes & Ladeira 1996a, 1996b). The pullout box is 1.53 m long, 1.00 m wide and 0.80 m deep (internal dimensions). To minimise the frictional effects of the front wall, a 0.20 m long sleeve is installed inside the box. The clamping system can be inserted into the test box through the sleeve, and thereby the initial unconfined length of the geosynthetic specimens is negligible. The normal stress is applied through a wooden plate loaded by ten small hydraulic jacks and is controlled by a load cell. A smooth neoprene sheet (0.025 m thick) is positioned between the top soil layer and the loading plate to attenuate the top boundary-soil friction and obtain more uniform distribution of the normal

stress. The tests are driven by a closed-loop servo-hydraulic control system that can accurately measure and control the loads and displacements. The applied pullout force is recorded by a load cell, whereas the geosynthetic frontal displacement is monitored by a linear potentiometer. The displacements along the length of the reinforcement are measured by means of inextensible wires fixed to the geosynthetic, with the opposite ends connected to linear potentiometers installed at the back of the pullout box. Test results are recorded by an automatic data acquisition system. Further details about the apparatus and test procedures can be found elsewhere (Lopes & Ladeira 1996a, 1996b, Ferreira et al. 2016, 2020a, 2020b, Vieira et al. 2020b).

2.2 Materials

A locally available granite residual soil often used as backfill material in Northern Portugal was selected for this current study. This soil can be classified as SW-SM (well-graded sand with silt and gravel) according to the Unified Soil Classification System. The main physical properties and the particle size distribution curve of this particular soil are presented in Table 1 and Figure 1, respectively.

The geosynthetic used was a uniaxial extruded geogrid manufactured from high-density polyethylene, HDPE (Figure 2). The physical and mechanical properties of this geogrid are listed in Table 2.

Table 1. Physical and mechanical properties of the granite residual soil.

Property	Value	Unit
D_{10}	0.09	mm
D_{30}	0.35	mm
D_{50}	1.00	mm
D_{60}	1.47	mm
C_U	16.90	-
C_C	1.00	-
G	2.73	-
γ_{dmax}	18.1	kN/m ³
γ_{dmin}	13.4	kN/m ³
$\phi' (I_D = 50\%)^1$	44.7	degree
$c' (I_D = 50\%)^1$	7.8	kPa
$\phi' (I_D = 85\%)^1$	46.6	degree
$c' (I_D = 85\%)^1$	29.5	kPa

¹ Obtained from large-scale direct shear tests (Ferreira et al. 2015).

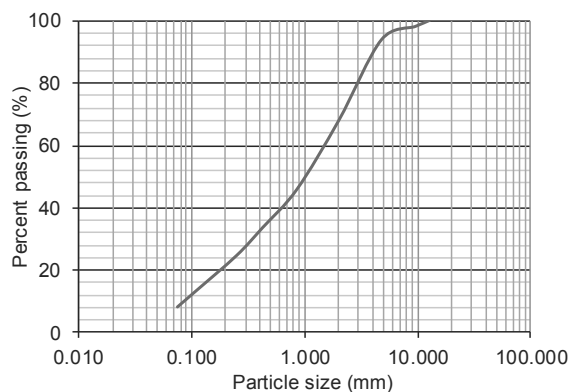


Figure 1. Soil particle size distribution curve.



Figure 2. Instrumented geogrid specimen installed over compacted soil.

Table 2. Physical and mechanical properties of the geogrid.

Property	Value	Unit
Raw material	HDPE	-
Mass per unit area	450	g/m ²
Mean aperture size	16×219	mm
Thickness of transverse ribs	2.7	mm
Thickness of longitudinal ribs	1.1	mm
Short term tensile strength ¹	52.2	kN/m
Strain at maximum load ¹	12.4	%
Short term tensile strength ²	68	kN/m
Strain at maximum load ²	11	%

¹ Obtained from tensile tests performed according to EN ISO 10319:2008 (CEN 2008) (machine direction).

² Provided by the manufacturer (machine direction).

2.3 Test program and loading characteristics

A series of multistage pullout tests was conducted to investigate the effects of cyclic loading on the geogrid pullout behaviour when embedded in the granite residual soil. Monotonic pullout tests were also performed for comparison purposes. All of the tests were carried out under a relatively low vertical pressure of 25 kPa to simulate low depths, where the pullout failure mechanism is most likely to occur in geosynthetic-reinforced soil systems.

The multistage pullout tests consisted of three different phases (Figure 3). Initially, a constant load increment rate of 0.2 kN/min (≈ 0.7 kN/m/min) was imposed until the pullout force reached 50% of the maximum pullout resistance obtained in the respective monotonic test (stage 1). A sinusoidal cyclic tensile load of constant frequency (f) and amplitude (A) was then applied (stage 2) for 40 cycles. Thereafter, the test proceeded again under constant load increment rate until the maximum pullout force was reached (stage 3). These tests were conducted under varying loading frequencies ($f = 0.01, 0.1$ and 1 Hz) and amplitudes ($A/P_R = 0.15, 0.40$ and 0.60 , where P_R is the maximum pullout force obtained in the corresponding monotonic test). The monotonic tests were also performed under load-controlled mode, using a constant load increment rate of 0.2 kN/min until the maximum pullout resistance was attained.

To investigate the influence of soil relative density (I_D) on the reinforcement pullout response, both the multistage and the monotonic tests were performed with medium dense soil (i.e., $I_D = 50\%$) and dense soil (i.e., $I_D = 85\%$).

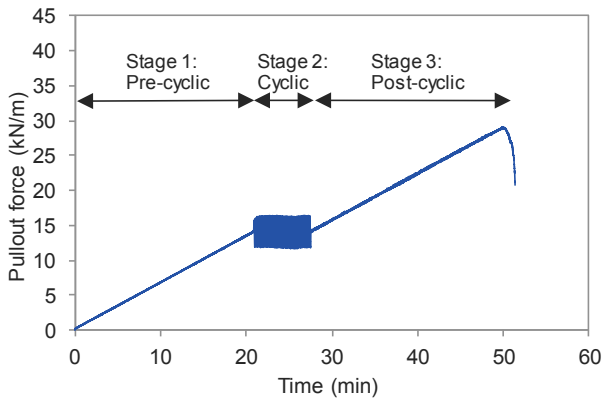


Figure 3. Evolution of pullout force with time from one representative test showing the different stages of the pullout tests.

3 RESULTS AND DISCUSSION

3.1 Pullout force-displacement behaviour

Figure 4 illustrates the evolution of the pullout force with the frontal displacement of the geogrid recorded during monotonic and multistage tests conducted under different conditions of soil density ($I_D = 50\%$ and $I_D = 85\%$). Figures 4a, 4b and 4c show the results obtained under a constant load amplitude ($A/P_R = 0.15$) and varying frequencies ($f = 0.01, 0.1$ and 1 Hz, respectively), whereas Figure 4d presents the results corresponding to $f = 0.1$ Hz and a higher amplitude ($A/P_R = 0.60$).

The results clearly show that soil density is a key factor affecting the pullout behaviour of the geogrid. Indeed, the maximum pullout force obtained from the monotonic tests increased approximately 36.2% when the soil placement density varied from 50% to 85%, whereas the frontal displacement at maximum pullout load decreased 23.5%. It can also be observed that the interface failure mode changed from pullout to tensile failure with the increase in soil density. The fact that higher pullout resistance is reached at interfaces involving denser soils is usually attributed to the higher shear strength of such soils, as well as the increase in normal stress at the geosynthetic level resulting from restrained soil dilation. This finding highlights the importance of an effective compaction of the backfill materials of geosynthetic-reinforced soil structures.

Comparing the results from monotonic (benchmark) and multistage tests (i.e. involving cyclic loading), it becomes apparent that the pullout stiffness of the reinforcement during the pre-cyclic stage of the multistage tests was rather similar to that attained in the corresponding monotonic test, denoting adequate repeatability of results (Figure 4). It is noteworthy that the test conditions imposed during the pre-cyclic stage were identical to those of the monotonic tests.

The results in Figure 4 also show that the geogrid frontal displacements increased throughout the cyclic loading stage, with the magnitude of such displacements depending upon the loading frequency and amplitude. A more detailed analysis of the cumulative cyclic displacements of the geogrid is presented later in this paper (Section 3.2).

When the soil was tested under medium dense conditions ($I_D = 50\%$), the cyclic loading histories generally led to a reduction in the maximum pullout resistance (P_R) of the geogrid recorded in the post-cyclic stage. The maximum reduction in P_R (20.4%) was obtained in the multistage test carried out under the highest frequency of 1 Hz (Figure 4c). Conversely, for $I_D = 85\%$ the maximum pullout resistance reached in the multistage tests did not significantly change comparatively to that attained under monotonic loading conditions. However, the frontal displacement at maximum pullout load was consistently higher in the multistage tests. The maximum increase relatively to the

monotonic test (48%) was attained in the test involving the highest cyclic loading amplitude of $A/P_R = 0.60$ (Figure 4d).

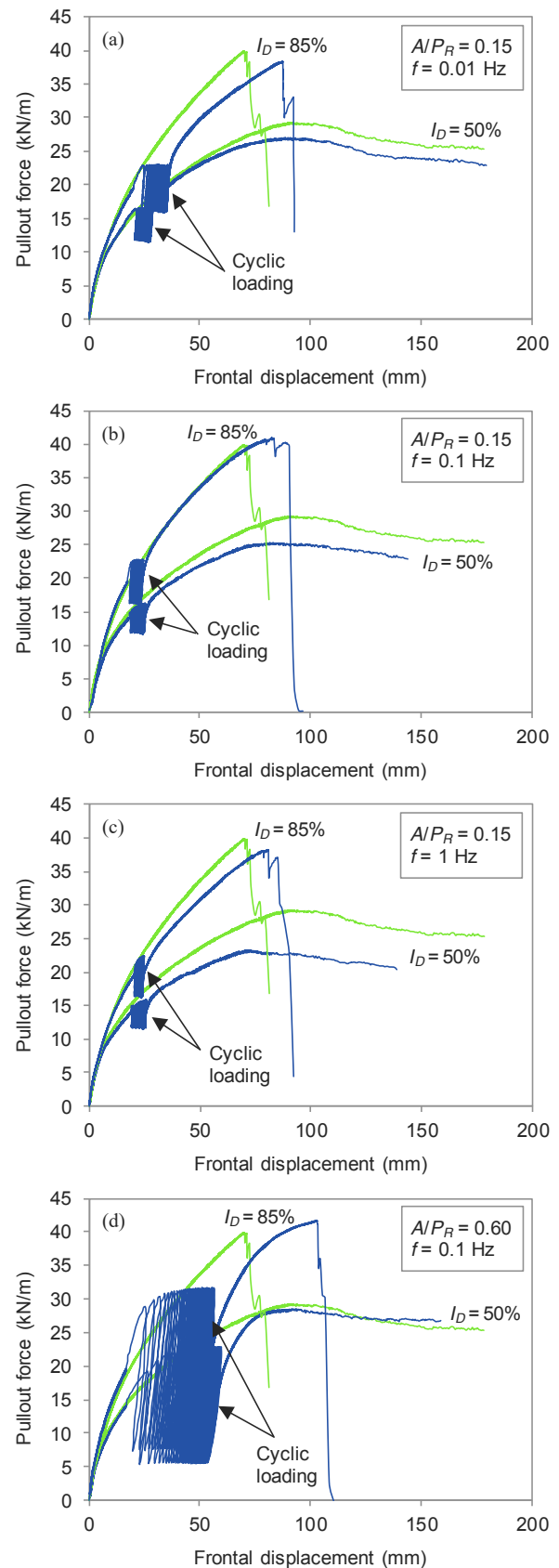


Figure 4. Evolution of pullout force with frontal displacement: (a) $A/P_R = 0.15, f = 0.01$ Hz; (b) $A/P_R = 0.15, f = 0.1$ Hz; (c) $A/P_R = 0.15, f = 1$ Hz; (d) $A/P_R = 0.60, f = 0.1$ Hz.

3.2 Deformative behaviour of the geogrid

The displacements recorded by the potentiometers over the geogrid length at the beginning and at the end of the cyclic loading phase (pre-cyclic and post-cyclic displacements, respectively) in tests involving medium dense and dense soil are shown in Figure 5. Figures 5a to 5c plot the displacement profiles associated with a fixed loading amplitude ($A/P_R = 0.15$) and increasing frequency ($f = 0.01 - 1$ Hz), whereas Figure 5d illustrates the results obtained under $f = 0.1$ Hz and $A/P_R = 0.60$.

As expected, the displacements decreased gradually throughout the geogrid length, which is attributed to the extensible nature of the reinforcement and the development of progressive failure mechanisms at the soil-geogrid interface.

The pre-cyclic displacements along the geogrid were generally similar for both soil relative densities, which can be explained by the fact that the frontal displacements at the onset of the cyclic loading stage were generally comparable in the tests performed with looser and denser soil, despite the differences in the magnitude of the corresponding pullout force.

For $I_D = 50\%$, the displacements increased over the whole geogrid length during cyclic loading, irrespective of the loading characteristics, implying that the whole geogrid length was mobilised. However, for $I_D = 85\%$, the displacements measured at the rear section of the geogrid were negligible under $A/P_R = 0.15$ and $f = 0.1$ Hz or 1 Hz (Figures 5b, 5c). The results also indicate that for a given soil density, the cyclic load-induced displacements along the reinforcement were more pronounced under higher amplitudes and lower frequencies. In fact, the cumulative cyclic displacement at the front end of the geogrid increased substantially (from 8.3 mm to 38.4 mm for $I_D = 50\%$, and from 6.4 mm to 33.7 mm for $I_D = 85\%$) with the increase in loading amplitude from $0.15P_R$ to $0.60P_R$ (Figures 5b, 5d). On the other hand, the increase in frequency from 0.01 to 1 Hz (Figures 5a to 5c) led to a reduction in the cumulative frontal displacement of the reinforcement (from 11.7 mm to 4.5 mm for $I_D = 50\%$, and from 15.1 mm to 4.0 mm for $I_D = 85\%$).

Figure 6 presents the evolution of displacements at the front and rear ends of the geogrid over the number of cycles for the different test conditions investigated in this study. It should be noted that these displacements were measured at the maximum pullout force for any specific number of load cycles. The effect of frequency on the displacements accumulated during cyclic loading is shown in Figures 6a and 6b, whereas the effect of amplitude is illustrated in Figures 6c and 6d.

In general, the cumulative displacements at either end of the geogrid increased with the number of cycles at a progressively decreasing rate, denoting progressive stabilisation of the interface response. However, such a stable condition under cyclic loading might be unacceptable if the accumulated displacements exceed the maximum admissible displacement for the serviceability limit state. Based on the criteria established by Allen and Bathurst (2002), a reference displacement of 30 mm is taken herein as the maximum allowable cumulative displacement, beyond which a medium-height geosynthetic-reinforced soil structure constructed with a granular backfill can be considered to exhibit poor performance.

Figure 6a indicates that the cumulative frontal displacement decreased progressively with increasing frequency, regardless of soil density. The effect of frequency on the displacements measured at the free end followed a similar trend, even though these displacements were relatively small, particularly for $I_D = 85\%$ (Figure 6b).

As shown in Figures 6c and 6d, the cyclic loading amplitude played a major role in the cumulative displacements of the reinforcement. The incremental displacements at both the front and rear ends of the geogrid increased progressively with the loading amplitude, hence adversely affecting the interface stability. Under the highest amplitude ratio ($A/P_R = 0.60$), the accumulated frontal displacements after 40 load cycles exceeded

the threshold value of 30 mm, irrespective of soil density (Figure 6c).

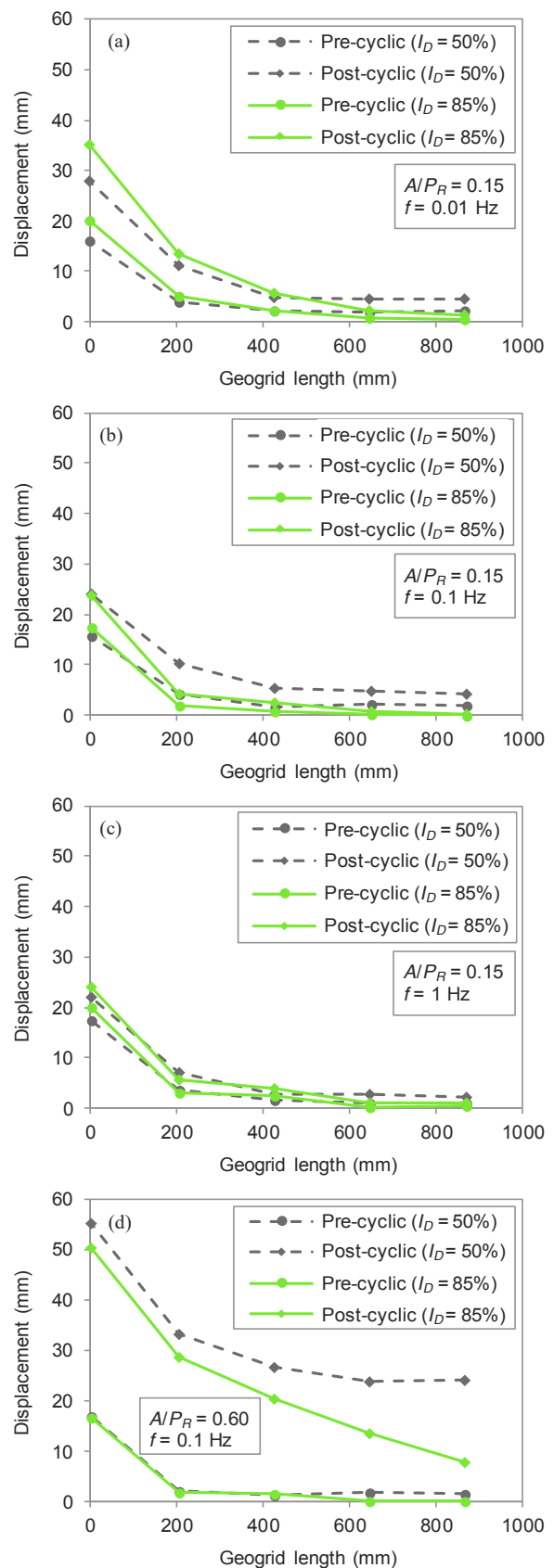


Figure 5. Measured pre- and post-cyclic displacements over the geogrid length: (a) $A/P_R = 0.15, f = 0.01$ Hz; (b) $A/P_R = 0.15, f = 0.1$ Hz; (c) $A/P_R = 0.15, f = 1$ Hz; (d) $A/P_R = 0.60, f = 0.1$ Hz.

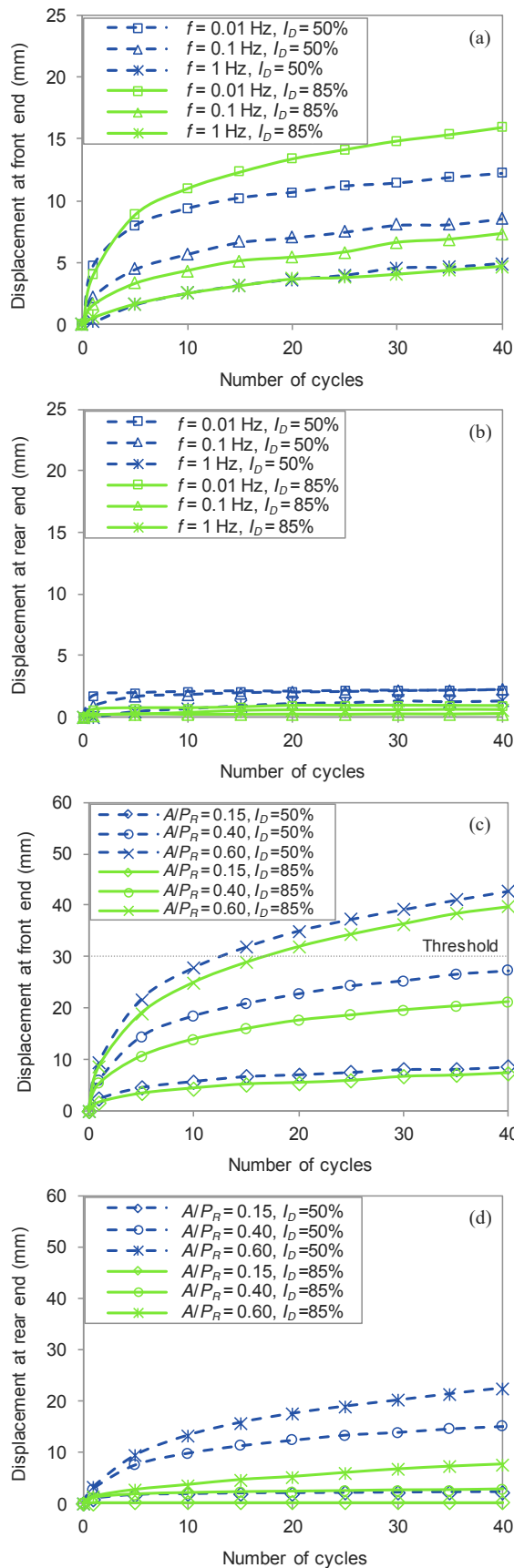


Figure 6. Cumulative cyclic displacements of the geogrid: (a)(b) effect of loading frequency for $A/P_R = 0.15$; (c)(d) effect of loading amplitude for $f = 0.1$ Hz.

Figures 6b and 6d also show that the displacements developed over the number of cycles at the free (rear) end of the reinforcement were consistently lower in the presence of dense soil, implying that soil density tends to restrain the transfer of shear stresses along the reinforcement length. This effect was particularly noticeable when higher amplitudes were imposed (Figure 6d).

Although the pullout trigger condition (i.e. the movement of the last geogrid transverse rib) was reached in several tests during the cyclic loading stage, no interface failure due to cyclic loading occurred for the test conditions investigated in this study.

4 CONCLUSIONS

The pullout response of a uniaxial extruded geogrid in a locally-available granite residual soil under cyclic and post-cyclic loading conditions was assessed through a series of large-scale pullout tests involving different conditions of soil density, cyclic loading amplitude (A) and frequency (f). The following conclusions can be derived from the results obtained in this study.

- The pullout resistance and deformation behaviour of the geogrid were highly influenced by the soil relative density (I_D). For $I_D = 50\%$ (medium dense soil), the cyclic loading histories generally induced a significant reduction in the geogrid pullout resistance, P_R (up to 20.4%), in comparison to that attained under monotonic loading conditions. In contrast, for $I_D = 85\%$ (dense soil), the peak pullout load reached during the post-cyclic stage was comparable to that obtained in the corresponding monotonic test.

- Regardless of soil density, the displacements measured throughout the reinforcement length during cyclic loading increased significantly with the loading amplitude and decreased with the increase in frequency.

- In general, the displacements recorded at either end of the geogrid during the cyclic stage increased with the number of cycles at a progressively decreasing rate, denoting stable soil-geogrid interface behaviour. However, under the highest amplitude ratio ($A/P_R = 0.6$), the cumulative cyclic displacements exceeded the threshold value of 30 mm, beyond which a medium-high geosynthetic-reinforced soil structure constructed with a granular backfill can be considered to exhibit marginal performance.

- For the conditions investigated, no soil-geogrid interface failure occurred during cyclic loading, regardless of the cyclic loading pattern and soil placement density.

5 ACKNOWLEDGEMENTS

This work was financially supported by: Project PTDC/ECI-EGC/30452/2017 - POCI-01-0145-FEDER-030452 - funded by FEDER funds through COMPETE2020 - Programa Operacional Competitividade e Internacionalização (POCI) and by national funds (PIDDAC) through FCT/MCTES; Programmatic funding - UIDP/04708/2020 of the CONSTRUCT - Instituto de I&D em Estruturas e Construções - funded by national funds through the FCT/MCTES (PIDDAC). The first author wishes to acknowledge the financial support from the Portuguese Foundation for Science and Technology (FCT) under Grant SFRH/BD/72886/2010.



6 REFERENCES

- Allen, T.M. and Bathurst, R.J. 2002. Observed long-term performance of geosynthetic walls and implications for design. *Geosynthetics International* 9(5-6), 567-606.
- Cardile, G., Pisano, M. and Moraci, N. 2019. The influence of a cyclic loading history on soil-geogrid interaction under pullout condition. *Geotextiles and Geomembranes* 47(4), 552-565.
- CEN 2008. EN ISO 10319:2008. Wide-width tensile tests. European Committee for Standardization, Brussels, Belgium.
- Farrag, K., Acar, Y.B. and Juran, I. 1993. Pull-out resistance of geogrid reinforcements. *Geotextiles and Geomembranes* 12(2), 133-159.
- Ferreira, F.B., Vieira, C.S. and Lopes, M.L. 2015. Direct shear behaviour of residual soil-geosynthetic interfaces-influence of soil moisture content, soil density and geosynthetic type. *Geosynthetics International* 22(3), 257-272.
- Ferreira, F.B., Vieira, C.S. and Lopes, M.L. 2020a. Pullout behavior of different geosynthetics - Influence of soil density and moisture content. *Frontiers in Built Environment* 6(12), 1-13.
- Ferreira F.B., Vieira, C.S., Lopes, M.L. and Carlos, D.M. 2016. Experimental investigation on the pullout behaviour of geosynthetics embedded in a granite residual soil. *European Journal of Environmental and Civil Engineering* 20(9), 1147-1180.
- Ferreira, F.B., Vieira, C.S., Lopes, M.L. and Ferreira, P.G. 2020b. HDPE geogrid-residual soil interaction under monotonic and cyclic pullout loading. *Geosynthetics International* 27(1), 79-96.
- Huang, B. and Bathurst, R.J. 2009. Evaluation of soil-geogrid pullout models using a statistical approach. *Geotechnical Testing Journal*, 32(6).
- Khedkar, M.S. and Mandal, J.N. 2009. Pullout behaviour of cellular reinforcements. *Geotextiles and Geomembranes* 27(4), 262-271.
- Lopes, M.L. and Ladeira, M. 1996a. Influence of the confinement, soil density and displacement rate on soil-geogrid interaction. *Geotextiles and Geomembranes* 14(10), 543-554.
- Lopes, M.L. and Ladeira, M. 1996b. Role of specimen geometry, soil height and sleeve length on the pull-out behaviour of geogrids. *Geosynthetics International* 3(6), 701-719.
- Mahigir, A., Ardakani, A. and Hassanlourad, M. 2021. Comparison between monotonic, cyclic and post-cyclic pullout behavior of a PET geogrid embedded in clean sand and clayey sand. *International Journal of Geosynthetics and Ground Engineering* 7(1).
- Moraci, N. and Cardile, G. 2009. Influence of cyclic tensile loading on pullout resistance of geogrids embedded in a compacted granular soil. *Geotextiles and Geomembranes* 27(6), 475-487.
- Moraci, N. and Cardile, G. 2012. Deformative behaviour of different geogrids embedded in a granular soil under monotonic and cyclic pullout loads. *Geotextiles and Geomembranes* 32, 104-110.
- Moraci, N. and Giofrè, D. 2006. A simple method to evaluate the pullout resistance of extruded geogrids embedded in a compacted granular soil. *Geotextiles and Geomembranes* 24(2), 116-128.
- Moraci, N. and Recalcati, P. 2006. Factors affecting the pullout behaviour of extruded geogrids embedded in a compacted granular soil. *Geotextiles and Geomembranes* 24(4), 220-242.
- Palmeira, E.M. 2004. Bearing force mobilisation in pull-out tests on geogrids. *Geotextiles and Geomembranes* 22(6), 481-509.
- Raju, D.M. and Fannin, R.J. 1998. Load-strain-displacement response of geosynthetics in monotonic and cyclic pullout. *Canadian Geotechnical Journal* 35(2), 183-193.
- Tran, V.D., Meguid, M.A. and Chouinard, L.E. 2013. A finite-discrete element framework for the 3D modeling of geogrid-soil interaction under pullout loading conditions. *Geotextiles and Geomembranes* 37, 1-9.
- Vieira, C.S., Ferreira, F.B., Pereira, P.M. and Lopes, M.L. 2020a. Pullout behaviour of geosynthetics in a recycled construction and demolition material - effects of cyclic loading. *Transportation Geotechnics* 23, 100346.
- Vieira, C.S., Pereira, P.M., Ferreira, F.B. and Lopes, M.L. 2020b. Pullout behaviour of geogrids embedded in a recycled construction and demolition material. Effects of specimen size and displacement rate. *Sustainability* 12(9), 3825.
- Weerasekara, L. and Wijewickreme, D. 2010. An analytical method to predict the pullout response of geotextiles. *Geosynthetics International* 17(4), 193-206.